Compressive Instabilities in Woven Textile Composites

Shunjun Song and Anthony M. Waas[1]
Department of Aerospace Engineering,
University of Michigan,
Ann Arbor, MI 48109-2140

1. Introduction

Conventional fiber reinforced laminated composites are widely used in the aerospace, automobile, and other industries. While they offer significant weight savings, relative disadvantages are manufacturing cost and through the thickness mechanical properties. Textile composites offer the potential to alleviate these disadvantages. Consequently, the in-plane mechanical properties of a wide variety of textile composites have been and continue to be an important area of research. During the past several decades, many researchers have developed numerous models to study textile composites. In the early eighties, Ishikawa and Chou[1] developed a "mosaic model" for analysis of elastic behavior of woven composites. Later, a 1D model referred to as the "fiber undulation model" was proposed by the same team[2]. Subsequently, several mechanics based models for predicting the elastic properties of woven composites were presented in [3-9] and several developments are summarized in the textbook by Chou[3].

Recently, Quek et al.[10,11,12] investigated the response and failure of a representative unit cell of a 2D triaxially braided composite under uniaxial compression, and also under multi-axial loads. They obtained good agreement on the predicted elastic constants and the maximum compressive strength compared against experiment. In this project, the behavior of 2D woven composite materials is investigated. Two aspects are studied. The first is the development of an analytical model to calculate the in-plane macroscopic elastic properties, E_x (Young's modulus in the x direction), E_y (Young's modulus in the y direction), G_{xy} (shear modulus in the x-y plane), and υ_{xy} (Poisson's ratio in the x-y plane), and the second is to establish the compressive response of a Representative Unit Cell (RUC) and its relation to the response of a collection of unit cells (multi-unit cells). The Representative Unit Cell (RUC) is the smallest repeating geometrical entity in the textile composite material. Figure 1 shows the microstructure of the RUC studied. The analytical results obtained from the first task are compared against the results from a 3D finite element (FE) analysis of the corresponding unit cell. This comparison establishes confidence in the analytical model. Results for the compressive response of a single RUC are compared to that of a nine RUC model in order to establish the salient features associated with the compression behavior. Details of the analytical model, which is similar to that reported in Quek et al.[10], are reported elsewhere.

2. Computational Model

Several analytical models for studying the response of textile composites are available[3] and many of these are based on some form of averaging (homogenization of the complex textile architecture). They are useful for obtaining the linear stiffnesses, but are not useful for establishing the compressive response, which involves both, geometric nonlinearity, and material nonlinearity associated with the tows and the polymer matrix material. Consequently, a fully 3D FE approach is pursued to establish the compressive response.

2.1 Model development

This 3D FE model consists of three components: 0° fiber tow, 90° fiber tow, and the polymer matrix. Each fiber tow has waviness in the $x'-z'$ plane as shown in Figure 2.

The waviness is a function of x', and is given as $z' = -0.014245(x'-7.015)^2 + 0.701$ with origin o' located at the left bottom corner as shown. A is the waviness amplitude and has a value 0.701mm. These geometrical features are taken into consideration in SDRC IDEAS MASTER SERIES 9.0 when creating the FE meshes. In all the meshes, 3D solid 10-noded tetrahedral elements were used. After creating the mesh, ABAQUS/Standard 6.3 was used to conduct the FE analysis. Due to geometric nonlinearity, it is necessary to ensure that the fiber tows are transversely isotropic in the current deformed configuration.

---

[1] Graduate Student Research Assistant and Professor, respectively.

This was achieved by using an inbuilt subroutine during the course of the analysis. Two configurations of the composite are considered; a single RUC and a nine RUC model.

2.2 Model properties

The FE models created were subjected to simple uniaxial and shear load states. In the single RUC case, convergence of the results with respect to mesh density was checked by evaluating the elastic constants as a function of the number of elements. The Young's modulus E_x, shear modulus G_{xy}, and Poisson's ratio υ_{xy} were computed. Figure 3 and Figure 4 show convergence of the computed G_{xy} and E_x, as a function of the number of elements. From the results shown, mesh size D containing 24144 elements was chosen for subsequent studies related to the nonlinear compression response. Table 1 shows the computed results for E_x. The results from both FE and the analytical model are listed for comparison. Note that in Table 1, results from another model (iso-tress for both steps) are also included.

2.3 Model implementation – boundary conditions

The boundary conditions used during the nonlinear response analysis and the simple load cases studied to obtain the elastic constants are shown in Figure 5 and Figure 6. Two types of boundary conditions as shown in Figure 5, were implemented. In the first case, during deformation the sides of the RUC are constrained to remain flat and move out uniformly while symmetric boundary conditions are used on the x-y planes. In the second case, the sides are unconstrained and are left free while symmetric boundary conditions are used on the x-y planes. It was found that the value of the elastic constant, E_x, reported in Table 1, is independent of the type of the boundary condition used. For the response analyses, it is the second type (sides free) of boundary condition that was used, since the former produces a higher value for the maximum limit load as will be discussed. The different boundary conditions and loading schemes implemented in the extraction of the elastic constants are shown in Figure 5 and Figure 6.

3. Results and Discussion

Accurate predictions of the elastic engineering constants provide verification of the computational model. Two types of response analyses were conducted. In the first type, the perfect RUC compressive responses are compared (single RUC and a nine cell RUC). This comparison was done to establish the effects of the number of unit cells on the peak load and the post peak response. In the second set of analyses, the effect of initial geometrical imperfections on the compressive response was studied by comparing the responses of a nine RUC composite with and without imperfection. The compressive response analyses of the RUC models were carried out using the RIKS method[14] option in ABAQUS. This option allows the possibility of capturing unstable equilibrium solutions that are typical in complex compressive response studies of the sort carried out here.

Prior to performing this, the effect of mesh density (number of elements) was studied by analyzing the single RUC compressive response. Figure 7 shows the stress-strain results for a single RUC response as a function of mesh density (number of elements). It was deemed that beyond a mesh size with 24144 elements the salient features of the RUC response did not change appreciably, thus reflecting convergence. Thus, this mesh size (24144 elements per RUC, referred to as mesh D) was used for all studies for which results are reported. Based on that mesh, a comparison between a one RUC and nine RUC model under uniaxial compression was performed. The response results will be discussed subsequently.

In the 'perfect' RUC cases, the one RUC and nine RUC models are subjected to uniaxial compression loading under displacement control, using side free boundary conditions. For the 'imperfect' RUC cases, a two-step approach is adopted. In the first step, the eigen modes of the structure are found and the mode corresponding to the lowest eigen frequency is used to perturb the mesh. The amplitude of perturbation is left as a parameter and the RUC responses to a series of imperfection amplitudes are analyzed. In all cases, nonlinear geometry and nonlinear matrix material properties are incorporated and special care is taken to ensure that the principal material axes of the transversely isotropic undulating fiber tows are maintained properly in the current deformed configuration. The results obtained for the single RUC (perfect) uniaxial compressive response are representative of the features that are observed in the different responses studied in this paper and it is illustrative to examine the features of a typical compressive response, by examining this case. The uniaxial compressive response for this case can be understood by examining a typical Σ_x versus ε_x plot (Figure 8). Here Σ_x is macroscopic stress and is obtained by dividing the resultant reaction force on the loaded face by the initial undeformed area of the loaded face. ε_x is the normalized end-shortening and is obtained by dividing the specified end displacement by the initial undeformed length of the RUC in the direction of load application. Also shown in Figure 8 are

the deformed tows (with matrix elements removed from RUC for visual display) as a function of increasing load. Initially, the RUC responses display a relatively stiff linear behavior (point A in figure 8). The magnitude of the slope of this line is 2.096E+08 KPa and agrees well with the linear elastic stiffness given earlier. As seen in Figure 8, with continued loading, the RUC response becomes progressively nonlinear (B), and at a strain (ε_x) of approximately 0.025, a maximum stress (Σ_x) of 3.42 MPa is reached. The value of strain at this maximum or peak and the value of the corresponding stress itself are dependent on the magnitude of initial tow undulation, which is associated with the degree of misalignment of the zero degree tow along the load application direction. The progressive reduction in the macroscopic stiffness of the RUC is due to the geometrical nonlinearity associated with the tows and the material nonlinearity of the matrix. Indeed, as loading proceeds, the matrix material that is between the tows is required to support increasing amounts of shear stress. However, the equivalent stress-strain curve of the matrix[15] indicates that the matrix modulus decreases progressively as the stress increases. Thus, because of the interaction of these nonlinearities, the overall stiffness of the RUC progressively decreases leading to a limit load type of instability. In an experimental setting, this limit load can be interpreted as the maximum compressive strength of the composite. However, at this load (or even prior to this), other events, such as matrix cracking and separation of the tows from the matrix (matrix/tow debonding) can occur, which may lead to tows "popping out", as is characteristically seen in a compression experiment at failure[12]. The modeling of matrix cracking and tow/matrix separation requires knowledge of the matrix cracking toughness and the tow-matrix interface toughness. Since reliable data pertaining to these mechanisms are currently not available, they are not considered in the present study. Instead, matrix distributed cracking, for instance, is being modeled through the elastic-plastic stress-strain response of the matrix with the implicit assumption that such cracking induces plastic like behavior.

As can be seen in Figure 9, the response of a one RUC model and that of a nine RUC model are comparable in terms of peak load, but the post-peak behavior shows differences. These differences are due to the type of deformation localization which is dictated by the spatial homogeneity of the structure. In order to investigate this further, the effect of initial geometrical imperfections was studied. The results of the "perfect" vs. 'imperfect" nine RUC compressive responses are shown in Figure 10. An initial imperfection with a shape that corresponds to the first natural frequency with a perturbation amplitude of x% (perturbation size divided by the tow diameter) was used. A series of such imperfection values corresponding to 0.71%, 1.43%, 2.14%, 2.85%, and 3.56% were used and the responses are displayed in Figure 10. It is clearly seen that the response of the nine RUC's becomes progressively nonlinear after the initial linear stage. Also the response shows the value of the strain at the peak load, and the peak load itself is dependent on the magnitude of the added imperfection. After the peak load, the stress is decreasing along with the increasing strain, which displays post peak softening. What is remarkable is that the post peak load shows convergence to a near plateau value while the peak load is continuously dependent on the imperfection magnitude.

4. Concluding Remarks

An iso-stress model in conjunction with CLT has been used to compute the elastic constants for a woven composite. The elastic constants found are in reasonable agreement with a fully 3D FE model of the RUC. The effect of the number of RUC's on the compressive response has been studied and it is found that the compressive strength obtained from a single RUC model is comparable to the nine RUC model, but the post peak response show differences. The effect of initial geometric imperfections on the compressive response has been studied for the nine RUC model. It is found that as expected, the compressive strength diminishes with increasing imperfection magnitude but the post-peak response shows convergence to a well defined plateau value.

5. References

1. Ishikawa, T. and Chou, T.W., Elastic behavior of woven hybrid composites. Journal of Composite Materials, 1982, 16(1), 2-19.
2. Ishikawa, T. and Chou, T.W., One-dimensional micromechanical analysis of woven fabric composites. AIAA Journal, 1983, 21(12), 1714-1721.
3. Chou, T.W., (1992), "Microstructural design of fiber composites", Cambridge Solid State Science Series
4. Miravete, A., (1999), "3-D textile reinforcements in composite materials", Woodhead Publishing Limited
5. Whitcomb, J.M., and Noh, J., (2000), "Concise Derivation of Formulas for 3D Sublaminate Homogenization", Journal of Composite Materials, 34, pp 522-535

6.   Naik, N.K., and Stembekar, P.S., (1992), "Elastic Behaviour of Woven Fabric Composites: I – Lamina Analysis", Journal of Composite Materials, 26, pp 2196-2225
7.   Huang, Z.M., (2000), "The mechanical properties of composites reinforced with woven and braided fabrics", Composite Science and Technology, 60, pp 479-498
8.   Naik, R., (1996), "Analysis of 2D triaxial and 3D multi-interlock braided textile composites", 37th AIAA / ASME / ASCE / AHS / ASC Structures, Structural Dynamics and Materials Conference
9.   Cox, B.N., and Dadkhah, M.S., (1995), "The macroscopic elasticity of 3D woven composites", Journal of Composite Materials, 29, pp 785-819
10.   Quek, S.C., Waas, A.M., Shahwan, K.W., Agaram, V., "Analysis of 2D triaxial flat braided textile composites", International Journal of Mechanical Sciences, 2003, 45, 1077-1096.
11.   Quek SC, Waas AM, Shahwan KW and Agaram, V. Compressive response and failure of braided textile composites: Part 2 – computations, Int J. Nonlinear Mech. 39 (4): 650-663, June 2003.
12.   Quek SC, Waas AM, Shahwan KW and Agaram, V. Compressive response and failure of braided textile composites: Part 1 - experiments, Int J. Nonlinear Mech. 39 (4): 635-648 June 2003.
13.   Reddy J.N., (1996), "Mechanics of Laminated Composite Plates: Theory and Analysis", CRC Press
14.   Riks, E., (1972), "The Application of Newton's Method to the Problem of Elastic Stability", Journal of Applied Mechanics-Transactions of the ASME, 39, 1060-1065
15.   Quek, SC, (2002), "Compressive Response and Failure of Braided Textile Composites: Experiments and Analysis", PhD thesis, The University of Michigan
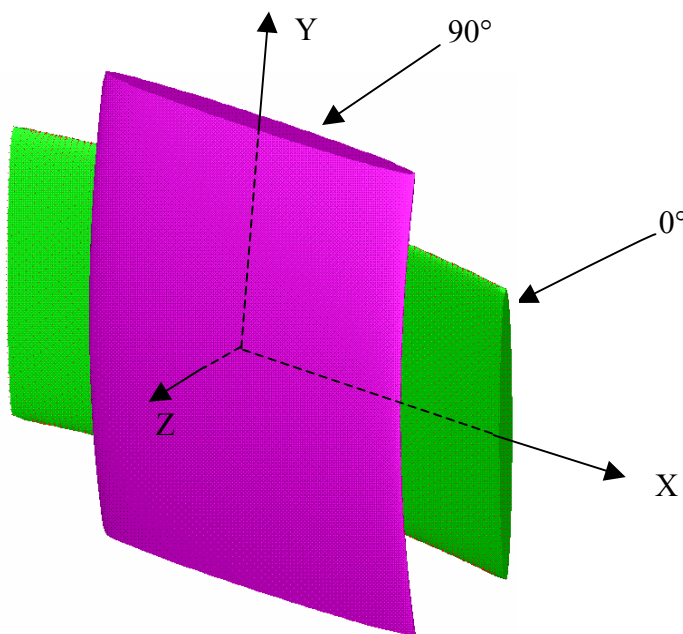
Figure 1: Microstructure of RUC fibers tows

Table 1 Comparison between results from analytical and FEM models for E_x

Averaging stage in $x'-z'$ plane	Iso-stress	Iso-stress	Iso-strain	FEM
Obtaining engineering constants	Iso-stress	Iso-strain	Iso-strain	FEM
Results(KPa)	1.3342E+07	2.3584E+08	2.729E+08	2.044E+08

Side Constrained

Side Free

(a)

(b)

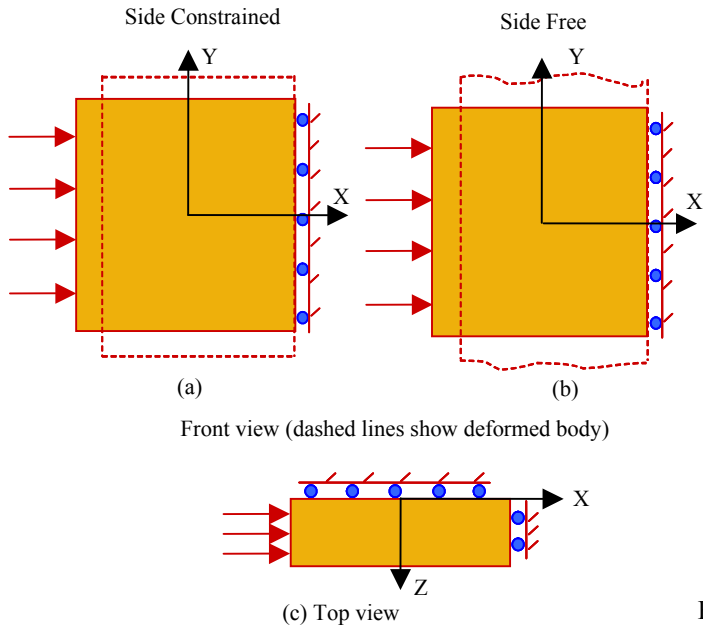Front view (dashed lines show deformed body)

(c) Top view

Figure 5 Loading and boundary conditions for the RUC analysis

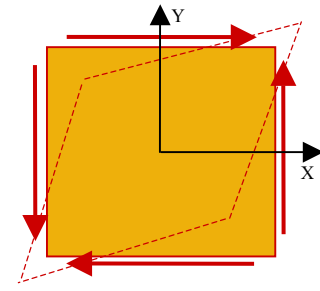Figure 6 Loading condition of RUC in the case of shear modulus in the x-y plane

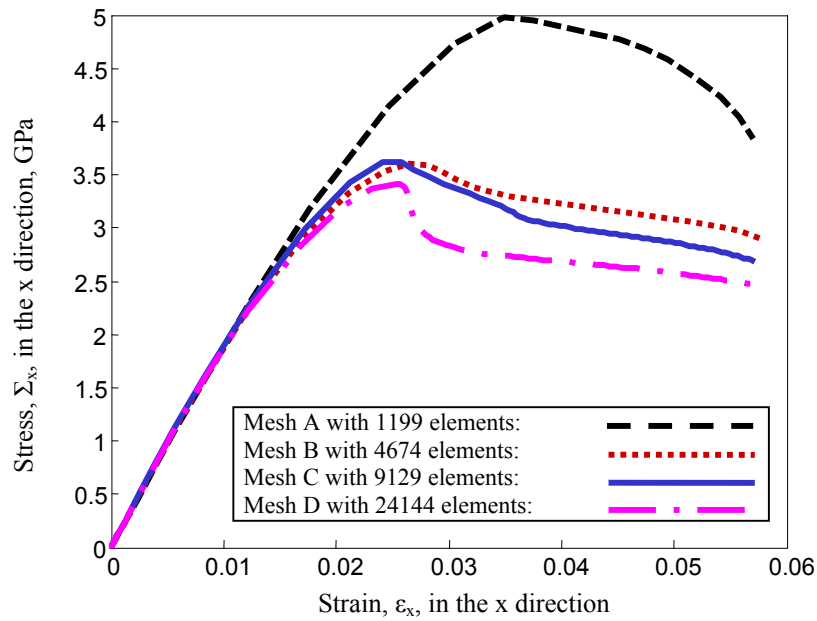Figure 7 Stress vs. Strain for One RUC with different mesh sizes

Mesh A with 1199 elements:
Mesh B with 4674 elements:
Mesh C with 9129 elements:
Mesh D with 24144 elements:

Stress, Σ_x, in the x direction, GPa

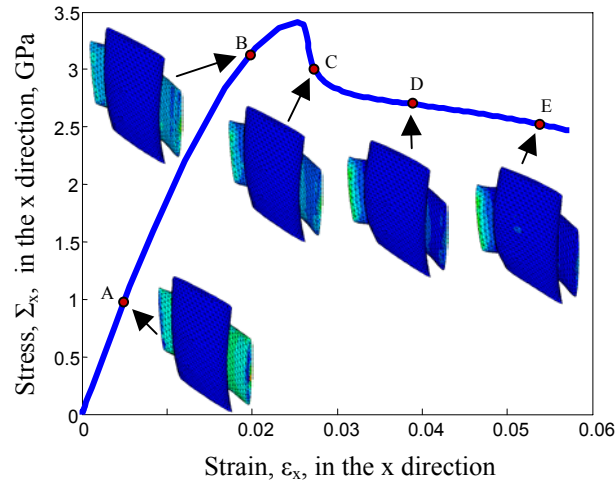Strain, ε_x, in the x direction

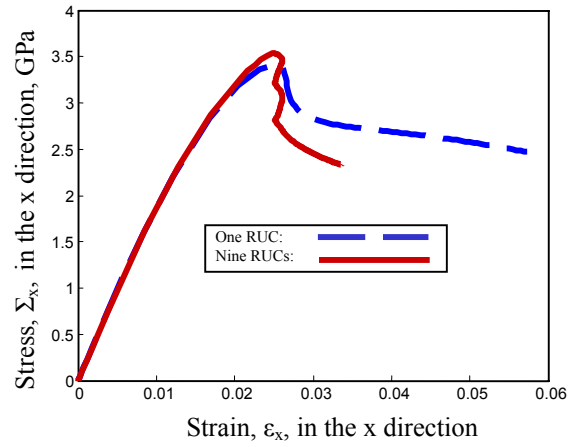Figure 8 Typical stress-strain response for a perfect one RUC model

Figure 9 Macroscopic stress-strain relation for a one RUC model compared against a nine RUC model
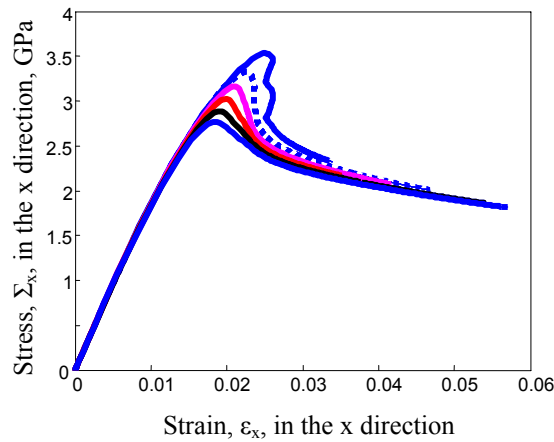

Figure 10 Macroscopic stress-strain relation as a function of initial geometric imperfection for a nine RUC composite